A Real Time Spectroscopic Probe of β-Hydrogen Transfer in the Gas Phase: Formation of $HFe(CO)_3(\eta^3\text{-}C_3H_5)$

Gregory T. Long, Wenhua Wang, and Eric Weitz*

Contribution from the Department of Chemistry, Northwestern University, Evanston, Illinois 60208-3113

Received May 12, 1995[⊗]

Abstract: Near-UV photolysis of a mixture of $Fe(CO)_5$ and C_3H_6 in the gas phase produces the (π-allyl) metal hydride complex, $HFe(CO)_3(\eta^3\text{-}C_3H_5)$, an intermediate implicated in iron carbonyl-catalyzed olefin isomerization. The formation of $HFe(CO)_3(C_3H_5)$ is rate limited by the addition of C_3H_6 to $Fe(CO)_3$ which has a rate constant of $(2.6 \pm 0.3) \times 10^{-10}$ cm^3 molecules^{-1} s^{-1} at 296 K. Subsequent to propene addition, the unimolecular rearrangement of $Fe(CO)_3(\eta^2\text{-}C_3H_6) \xrightarrow{k_1} HFe(CO)_3(\eta^3\text{-}C_3H_5)$ takes place with a lower bound for k_1 of 10^{10} s^{-1}. With the assumption of a preexponential for k_1 of 10^{13} s^{-1}, the activation enthalpy associated with k_1 is <3.5 kcal mol^{-1}. The data are consistent with the establishment of an equilibrium between $HFe(CO)_3(\eta^3\text{-}C_3H_5)$ and $Fe(CO)_3(\eta^2\text{-}C_3H_6)$ with an equilibrium constant of 2.4×10^{-5} and an isotope effect of $K_{eq}^H/K_{eq}^D = 0.45$ at 296 K. $Fe(CO)_3(C_3H_6)_2$ forms by addition of propene to $Fe(CO)_3(\eta^2\text{-}C_3H_6)$, which is in equilibrium with $HFe(CO)_3(\eta^3\text{-}C_3H_5)$, with a phenomenological rate constant $K_{eq}k_+ = (4.5 \pm 0.1) \times 10^{-16}$ cm^3 molecules^{-1} s^{-1}. A van't Hoff plot gives $\Delta H = 7.2 \pm 0.6$ kcal mol^{-1} and $\Delta S = 3 \pm 2$ cal K^{-1} mol^{-1} for the process $HFe(CO)_3(\eta^3\text{-}C_3H_5) \rightarrow Fe(CO)_3(\eta^2\text{-}C_3H_6)$, assuming that the rate constant for addition of C_3H_6 to $Fe(CO)_3(C_3H_6)$, k_+, is $\sim 1.6 \times 10^{-11}$ cm^3 molecules^{-1} s^{-1}. These results can be quantitatively related to a catalytic cycle for olefin isomerization.

I. Introduction

Studies of metal carbonyls have provided important information on organometallic reaction mechanisms,[1,2] in part, because the frequencies of the CO ligands are very sensitive to the electronic environment of the metal.[2] Coordinatively unsaturated metal carbonyls catalyze a variety of reactions including α-hydrogen transfer reactions such as C−H oxidative addition[3] and β-hydrogen transfer processes such as β-elimination[4] and olefin isomerization.[5] Additionally, coordinatively unsaturated metal carbonyls can be conveniently produced by near-UV photolysis.[6]

Hydrogen transfer processes are well-studied ligand transformations in organometallic chemistry,[7] which can occur both thermally[8] and photochemically,[9] and often necessitate the formation of a 16-electron species with an open coordination site on the metal center.[10] Yet, the apparently rapid rates for these processes have made elucidation of the details of hydrogen transfer mechanisms challenging.

Metal carbonyl-catalyzed olefin isomerization that proceeds by a (π-allyl) metal hydride mechanism[11] involves a hydrogen transfer process and also provides a setting for studying intramolecular C−H oxidative addition.

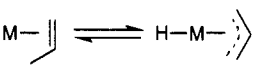

Early isotopic scrambling[12] and photochemical[13] studies invoked $HFe(CO)_3(\pi\text{-allyl})$ as the key intermediate in olefin isomerization. In an effort to directly observe such an intermediate, Mitchner and Wrighton photolyzed $Fe(CO)_4$(olefin) in a methylcyclohexane (MCH) matrix at 77 K and observed only the saturated $HFe(CO)_3(\pi\text{-allyl})$ complex when the olefins under study contained allylic H's (propene, pentene).[14] Photolysis of $Fe(CO)_4$(olefin) gives the unsaturated $Fe(CO)_3$(olefin) for olefins containing no allylic H's (ethylene and 3,3-dimethyl-1-pentene). Consistent with these results and a mechanism involving formation of a π-allyl metal hydride, Barnhart and McMahon observed direct intramolecular C−H bond insertion[15] on photolyzing $Fe(CO)_4(\eta^2\text{-}C_3H_6)$ in Ar and MCH matrices at 10 K. This process generates both $Fe(CO)_3(\eta^2\text{-}C_3H_6)$ and $HFe(CO)_3(\eta^3\text{-}C_3H_5)$. Even at 5 K, they observed facile thermal conversion of $Fe(CO)_3(C_3H_6)$ to $HFe(CO)_3(C_3H_5)$ indicating that $HFe(CO)_3(C_3H_5)$ is thermodynamically more stable.

[⊗] Abstract published in *Advance ACS Abstracts*, December 1, 1995.

(1) Howell, J. S.; Burkinshaw, P. M. *Chem. Rev.* **1983**, *83*, 557.
(2) Geoffroy, G. L.; Wrighton, M. S. *Organometallic Photochemistry*; Academic Press: New York, 1979.
(3) (a) Janowicz, A. H. Bergman, R. G. *J. Am. Chem. Soc.* **1982**, *104*, 352. (b) Hoyano, J. K.; Graham, W. A. G. *J. Am. Chem. Soc.* **1982**, *104*, 3723.
(4) (a) Kaslauskas, R. J.; Wrighton, M. S. *J. Am. Chem. Soc.* **1982**, 104, 6005. (b) Mahmoud, K. A.; Rest, A. J.; Alt, H. G.; Eichner, M. E.; Jansen, B. M. *J. Chem. Soc., Dalton Trans.* **1984**, 175. (c) Yang, G. K.; Peters, K. S.; Vaida, V. *J. Am. Chem. Soc.* **1986**, *108*, 2511.
(5) (a) Tolman, C. A. In *Transition Metal Hydrides*; Muetterties, E. L., Ed.; Dekker: New York, 1971; Vol. 1. (b) Keim, W. In *Transition Metals in Homogeneous Catalysis*; Schrautzer, G. N., Ed.; Dekker: New York, 1971. (c) Taqui Khan, M. M.; Martell, A. E. *Homogeneous Catalysis by Metal Complexes*; Academic: New York, 1974; Vol II. (d) Wrighton, M. S.; Ginley, D. S.; Schroeder, M. A.; Morse, D. L. *Pure Appl. Chem.* **1975**, *41*, 671.
(6) Weitz, E. *J. Phys. Chem.* **1987**, *91*, 3945.
(7) Collman, J. P.; Hegedus, L. S.; Norton, J. R.; Finke, R. G. *Principles and Applications of Organotransition Metal Chemistry*, 2nd ed.; University Science Books: Mill Valley, 1987.
(8) McGhee, W. D.; Bergman, R. G. *J. Am. Chem. Soc.* **1988**, *110*, 4246.
(9) Zhuang, J.; Sutton, D. *Organometallics* **1991**, *10*, 1516.
(10) Jordan, R. B. *Reaction Mechanisms of Inorganic and Organometallic Systems*; Oxford University Press: New York, 1991.
(11) Crabtree, R. H. *The Organometallic Chemistry of the Transition Metals*; Wiley-Interscience: New York, 1994.
(12) Casey, C. P.; Cyr, C. R. *J. Am. Chem. Soc.* **1973**, *95*, 2248.
(13) Schroeder, M. A.; Wrighton, M. S. *J. Am. Chem. Soc.* **1976**, *98*, 551.
(14) Mitchner, J. C.; Wrighton, M. S. *J. Am. Chem. Soc.* **1983**, *105*, 1065.
(15) Barnhart, T. M.; McMahon, R. J. *J. Am. Chem. Soc.* **1992**, *114*, 5434.

0002-7863/95/1517-12810$09.00/0

A powerful method for monitoring transient species in real time employs UV-laser photolysis and time-resolved IR spectroscopy.[16] Over the last decade this technique has greatly increased the existing body of knowledge on the reactive behavior of metal carbonyls and more recently has been applied to determine bond energies in systems of ligands weakly bound to coordinatively unsaturated metal carbonyls.[16,17] While, to our knowledge, there have been no detailed kinetic studies of metal carbonyl-photocatalyzed olefin isomerization, a number of reports address the related hydrogen transfer processes of β-elimination and intermolecular C−H bond activation. A study of β-elimination in $CpM(CO)_3Et$ (M = Mo, W) in heptane at room temperature led to the suggestion that β-hydrogen transfer is a facile process taking place without significant activation barriers.[18] Perutz and co-workers report the addition of alkanes, arenes, and olefins to $Fe(dmpe)_2$ in oxidative addition processes.[19] Bergman and co-workers studied the C−H bond activation of cyclohexane-d_0 and d_{12} and neopentane-d_0 and -d_{12} by photolysis of $Cp^*Rh(CO)_2$,

$$Cp^*Rh(CO)(alkane) \rightarrow Cp^*Rh(CO)(H)(alkyl)$$

in liquid rare gases.[20] They report rate constants of $k(193K) \sim 10^6$ s^{-1} and $k(193K) \sim 10^5$ s^{-1} for C_6H_{12} and $C(CH_3)_4$, respectively, and an activation energy of ~4 kcal mol^{-1} for C_6H_{12}. Hence, C−H activation in these systems is a facile process.

A potential concern involving reactions of coordinatively unsaturated species taking place in solution is that measured rates may be perturbed by coordination of solvent to an unsaturated metal center which can occur on a picosecond time scale.[21] The gas phase provides an environment in which fundamental kinetic and mechanistic processes can be studied in the absence of solvent effects. One of the few mechanistic studies involving C−H bond breaking in the gas phase is the work of Bergman and co-workers, who report the rate constant for intermolecular C−H oxidative addition of an alkane to CpRh(CO).[22] Interestingly, they did not observe the initial addition product, CpRh(CO)(alkane), observed in solution, but rather the oxidative addition product, CpRh(CO)(H)(alkyl). In this study, we report a gas-phase study of the kinetics and the mechanism of β-hydrogen transfer which is relevant to olefin isomerization and intramolecular C−H bond activation. Gas-phase photolysis of $Fe(CO)_5$ yields predominantly $Fe(CO)_3$, a naked multiply coordinatively unsaturated species, which can react with C_3H_6 leading to a π-allylic metal hydride ($HFe(CO)_3(C_3H_5)$) which is a proposed intermediate for olefin isomerization. The gas-phase photochemistry of $Fe(CO)_5$ is well understood.[23] Since propene is the simplest olefin that can form an allylic species, this study provides a model system in which intermediates present in systems undergoing olefin isomerization can be monitored. From the results obtained for this model system, a catalytic cycle for olefin isomerization is presented for which the kinetics and energetics of all steps have been measured or estimated.

II. Experimental Section

The apparatus used for transient absorption studies is described in detail elsewhere.[6,16,17] In a typical experiment, $Fe(CO)_5$, C_3H_6, and He are delivered to either a 15 × 2.5 cm (i.d.) static Pyrex cell or a 35 × 1.5 cm (i.d.) Pyrex flow cell terminated by CaF_2 windows. In static cell experiments, sample gas pressures are measured by a capacitance manometer (MKS). In flow cell experiments, $Fe(CO)_5$ is delivered by a needle valve and its pressure is estimated based on its absorbance. Other sample gases pass thorough calibrated mass flow controllers (Tylan) and the total cell pressure is monitored. For C_3H_6 pressures above 1 atm, a high-pressure cell was employed.[24] This cell consists of a 3.25 in. × 3 in. × 2 in. gold plated copper block with two perpendicular $^3/_8$ in. holes terminated by sapphire windows.

The photolysis source is the pulsed, unfocused output of an excimer laser (Questek 2110), running on either XeF (351 nm) or KrF (248 nm). The repetition rate of the laser is set so that the sample gases sweep out the volume of the flow cell between laser shots, typically 0.3 or 1.0 Hz. Fluences incident on the front window of the cell were ~6 mJ cm^{-2} for 248-nm photolysis and ~13 mJ cm^{-2} for 351-nm photolysis, as measured by a Scientec power meter. Prior studies have shown that photolysis of $Fe(CO)_5$ is a single photon process at these fluences.[25]

Three IR probe sources were employed in this study. FTIR spectra were collected with a Mattson RS-1 spectrometer operating at 4-cm^{-1} resolution. Experiments on the microsecond time scale employed either a home-built line-tunable liquid N_2-cooled CO laser or a tunable infrared diode laser (Laser Photonics). The CO laser was used for static cell experiments. The diode laser, with better long-term amplitude stability, was employed in virtually all flow cell experiments and some static cell experiments. The diode laser beam is collimated after passing through a 0.5-m monochromator (*f*/11 Czerny-Turner) which ensures single mode output. The probe beam was double-passed through the cell and its attenuation by photoproducts was monitored with a fast InSb detector (SRBC or Judson). The InSb detector was protected from UV radiation by a 4.5 μm LP filter on a Ge substrate. Minimum response times of the SBRC and Judson detectors were each determined to be ~70 ns, from single exponential fits of the detector-limited decay of $Fe(CO)_5$ upon photolysis. The detector output was amplified (Perry × 100 or SRS 560 × 100), digitized, signal averaged (Lecroy 9400), and stored and manipulated on a PC. Time-resolved spectra (4−6 cm^{-1} resolution) were constructed over the spectral region of interest from transient waveforms which were connected at common delay times.

Kinetic information was determined by collecting transients at a particular probe frequency as a function of the pressure of the reactant of interest. These transients were fit to exponentials using a fitting routine described by Provencher.[26] Except where otherwise noted, all reported rate constants were measured at 296 ± 2 K. All errors are reported as $\pm 2\sigma$, on the basis of linear regression fits.

Temperature variation between 274 and 309 K was achieved either by water-cooling a jacketed cell or by wrapping the cell with heating tape for temperatures below and above room temperature, respectively. Thermal equilibration between the sample gases and the cell was verified by thermocouples placed at the center and ends of the cell.

(16) Poliakoff, M.; Weitz, E. *Adv. Organomet. Chem.* **1986**, *25*, 277.
(17) Weitz, E. *J. Phys. Chem.* **1994**, *98*, 11256.
(18) Johnson, F. P. A.; Gordon, C. M.; Hodges, P. M.; Poliakoff, M.; Turner, J. J. *J. Chem. Soc., Dalton Trans.* **1991**, 833.
(19) Whittlesey, M. K.; Mawby, R. J.; Osman, R.; Perutz, R. N.; Field, L. D.; Wilkinson, M. P.; George, M. W. *J. Am. Chem. Soc.* **1993**, *115*, 8627.
(20) (a) Schultz, R. H.; Bengali, A. A.; Tauber, M. J.; Weiller, B. H.; Wasserman, E. P.; Kyle, K. R.; Moore, C. B.; Bergman, R. G. *J. Am. Chem. Soc.* **1994**, *116*, 7369. (b) Bengali, A. A.; Schultz, R. H.; Moore, C. B.; Bergman, R. G. *J. Am. Chem. Soc.* **1994**, *116*, 9585.
(21) (a) Simon, J. D.; Peters, K. S. *Chem. Phys. Lett.* **1983**, *98*, 53. (b) Wang, L.; Zhu, X.; Spears, K. G. *J. Am. Chem. Soc.* **1988**, *110*, 8695. (c) Wang, L.; Zhu, X.; Spears, K. G. *J. Phys. Chem.* **1989**, *93*, 2. (d) Joly, A. G.; Nelson, K. F. *J. Phys. Chem.* **1989**, *93*, 2876. (e) Joly, A. G.; Nelson, K. F. *Chem. Phys.* **1991**, *152*, 69. (f) Anfinrud, P. A.; Han, C.-H.; Lian, T.; Hochstrasser, R. M. *J. Phys. Chem.* **1991**, *95*, 574. (g) King, J. C.; Zhang, J. Z.; Schwartz, B. J.; Harris, C. B. *J. Chem. Phys.* **1993**, *99*, 7595. (h) Dougherty, T. P.; Heilweil, E. J. *J. Chem. Phys.* **1994**, *100*, 4006.
(22) Wasserman, E. P.; Moore, C. B.; Bergman, R. G. *Science* **1992**, *255*, 315.
(23) (a) Seder, T. A.; Ouderkirk, A. J.; Weitz, E. *J. Chem. Phys.* **1986**, *85*, 1977. (b) Ryther, R. J.; Weitz, E. *J. Phys. Chem.* **1992**, *96*, 2561.
(24) Moustakas, A.; Weitz, E. *J. Chem. Phys.* **1993**, *98*, 6947.
(25) Waller, I. M.; Hepburn, J. W. *J. Chem. Phys.* **1988**, *88*, 6658.
(26) Provencher, S. W. *Biophys. J.* **1976**, *16*, 27. Provencher, S. W. *J. Chem. Phys.* **1976**, *64*, 2772.

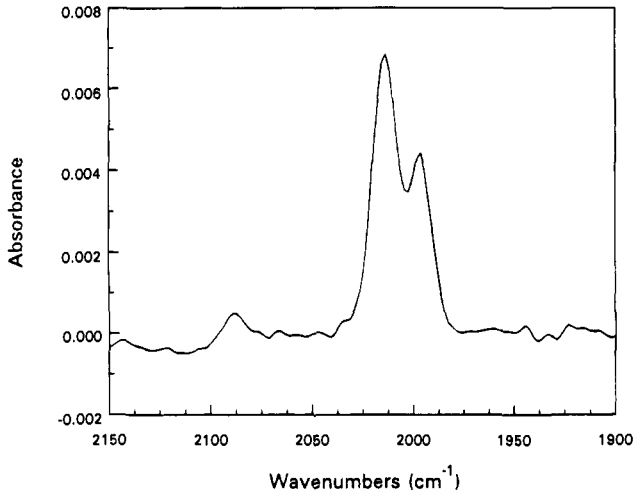

Figure 1. Gas-phase FTIR spectrum resulting from subtraction of the residual $Fe(CO)_5$ spectrum from the spectrum generated by 351-nm photolysis of a static cell fill of 50 mTorr of $Fe(CO)_5$, 50 Torr of C_3H_6, and 2 Torr of CO collected at 4-cm^{-1} resolution and 2000 scans.

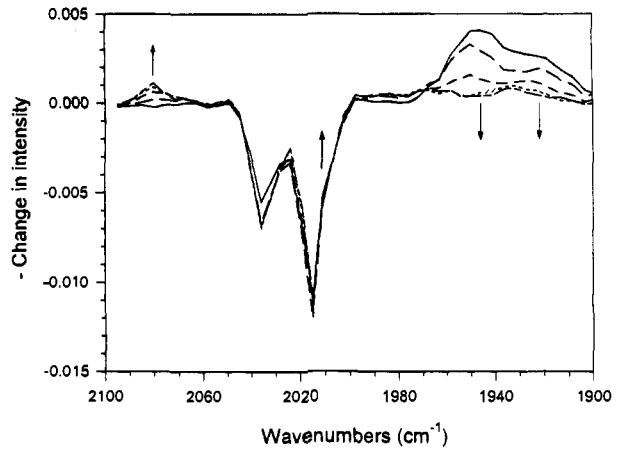

Figure 2. Time-resolved diode laser flow cell spectrum of ~5 mTorr of $Fe(CO)_5$, 190 mTorr of C_3H_6, and 13.4 Torr of He generated by 248-nm photolysis. The spectrum is shown in 0.6-μs increments for times of 0.6–3.0 μs. The solid trace marks the first increment. Arrows indicate the direction of the evolution of absorptions.

$Fe(CO)_5$ pressures of ~5 and ~30 mTorr were typical for 248- and 351-nm photolysis, respectively. Propene pressures were 50–500 mTorr for experiments which measured the rates of propene (C_3H_6 or C_3D_6) addition, 20–500 Torr for experiments probing the decay of $HFe(CO)_3(C_3H_5)$ and formation of $Fe(CO)_3(C_3H_6)_2$, and up to 11.4 atm for experiments which attempted to monitor the initial formation of $Fe(CO)_3(C_3H_6)_2$ or $Fe(CO)_3(C_3D_6)_2$. Helium, an efficient collisional relaxer of excited vibrational and rotational states, was used as a buffer gas to provide a third body to stabilize products in association reactions and thus to ensure that association reactions were measured in their "high-pressure" limit. Typical He pressures were 30 Torr for experiments directed toward measuring the rates of C_3H_6 addition and up to 500 Torr for experiments which probed the rate of decay of $HFe(CO)_3(C_3H_5)$.

$Fe(CO)_5$, obtained from Aldrich, was degassed prior to use by several freeze–pump–thaw cycles. C_3H_6 (99% purity) and C_2H_4 (99.5%) were obtained from Matheson, C_3D_6 (98% d_6) from Cambridge Isotope Laboratories, and He (99.999%) from Linde. All were used without further purification.

III. Results

The degree of coordinative unsaturation of iron carbonyls produced in the gas-phase photolysis of $Fe(CO)_5$ increases with photon energy.[23] $Fe(CO)_3$, the species of interest in this study, is the major photoproduct at both 351 and 248 nm. There were no detectable differences in the behavior of $Fe(CO)_3$ or its adducts subsequent to $Fe(CO)_3$ production by 351- or 248-nm photolysis of $Fe(CO)_5$/propene mixtures.

The 351- or 248-nm gas-phase photolysis of $Fe(CO)_5$ leads to the production of three distinct species as a result of reaction of $Fe(CO)_3$ and $Fe(CO)_4$ with propene. In static cell experiments, the concentration of the compound designated as species I can be built up with multiple laser shots and is sufficiently stable that its spectrum can be obtained with conventional FTIR. The FTIR spectrum in Figure 1, in which the residual parent absorption is substracted out for 50 mTorr of $Fe(CO)_5$ photolyzed in the presence of 50 Torr of C_3H_6 and 10 Torr of CO, reveals product bands for species I at 2089, 2014, and 1988 cm^{-1}. These features are consistent with bands at 2088, 2006, and 1988 cm^{-1} reported for $Fe(CO)_4(C_3H_6)$ in an Ar matrix.[15] The relatively long lifetime of $Fe(CO)_4(C_3H_6)$ is also consistent with literature reports that it is a stable species as a solid or in solution that can be synthesized with conventional[27] or photochemical[28] methods. Due to its stability, $Fe(CO)_4(C_3H_6)$ is not involved in the kinetic processes discussed in the remainder of this study. The addition of CO to a mixture of $Fe(CO)_5$ and C_3H_6 enhances the production of this species, however it forms even in the absence of added CO. Formation of $Fe(CO)_4(C_3H_6)$ can occur via a number of pathways. $Fe(CO)_4$, a primary product on 351-nm photolysis, can react with C_3H_6 to form $Fe(CO)_4(C_3H_6)$. $Fe(CO)_3$ generated via either 248- or 351-nm photolysis can react with CO either prior or subsequent to reaction with C_3H_6. Additionally, $Fe(CO)_4(C_3H_6)$ can form by the loss of propene from $Fe(CO)_3(C_3H_6)_2$ and subsequent addition of CO. It is also possible for $Fe(CO)_3(C_3H_6)$, which is present as part of the equilibrium shown in eq 3 (*vide infra*), to react with photolytically generated CO to produce $Fe(CO)_4(C_3H_6)$.

The 248- or 351-nm gas-phase photolysis of $Fe(CO)_5$, in the presence of C_3H_6, leads to the production of two common species in addition to $Fe(CO)_4(C_3H_6)$. A time-resolved IR diode laser flow cell spectrum for 248-nm photolysis of ~5 mTorr of $Fe(CO)_5$ in the presence of 190 mTorr of C_3H_6 and 13.4 Torr of He is displayed in Figure 2. At the earliest times, the detector-limited loss of $Fe(CO)_5$ and photoproduction of $Fe(CO)_3$ at 1950 cm^{-1} and $Fe(CO)_2$ at 1922 cm^{-1} are the dominant features. In the first two spectra, these product bands sharpen and blue shift, characteristic of the internal relaxation of primary photoproducts.[29] $Fe(CO)_3$ decays to the baseline over a 3.0-μs period, as a product grows in centered at 2080 cm^{-1} (species II). The slope of a plot of the pseudo-first-order rates for $Fe(CO)_3$ decay at 1953 cm^{-1} and product growth monitored at 2077 cm^{-1}, as a function of C_3H_6 pressure, yields a bimolecular rate constant for the addition of C_3H_6 to $Fe(CO)_3$ of $(2.6 \pm 0.3) \times 10^{-10}$ cm^3 $molecules^{-1}$ s^{-1} (Figure 3). Also present in Figure 2 is a band monitored at 2011 cm^{-1} which is partially obscured by the parent absorption that has the same C_3H_6 dependence as the band monitored at 2077 cm^{-1}. Virtually identical behavior is observed for these bands subsequent to 351-nm photolysis. Though there were some additional absorptions present on 248-nm photolysis relative to 351-nm photolysis, primarily in the 1900–1960-cm^{-1} region, presumably due to reactions of $Fe(CO)_2$ with propene, these features were not subjected to systematic study.

(27) Weiller, B. H.; Miller, M. E.; Grant, E. R. *J. Am. Chem. Soc.* **1987**, *109*, 352.

(28) Wuu, Y.; Bentsen, J. G.; Brinkley, C. G.; Wrighton, M. S. *Inorg. Chem.* **1987**, *26*, 530.

(29) Ouderkirk, A. J.; Seder, T. A.; Weitz, E. *Laser Applications to Industrial Chemistry*; SPIE: New York, 1984; Vol. 458, p 148.

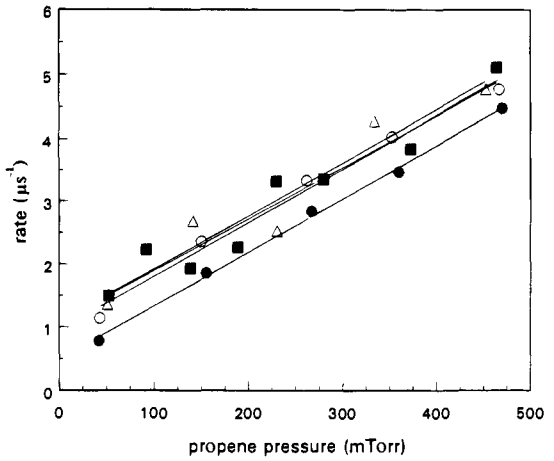

Figure 3. A plot of the pseudo-first-order rates at 296 K for addition of propene to $Fe(CO)_3$ as a function of propene pressure. The rates were monitored at 1953 cm1$-^1$ (disappearance of $Fe(CO)_3$) (○), 2077 cm^{-1} (formation of Species II) (■), 2011 cm^{-1} (formation of Species II) (△), and 1953 cm^{-1} (disappearance of $Fe(CO)_3$ using C_3D_6) (●).

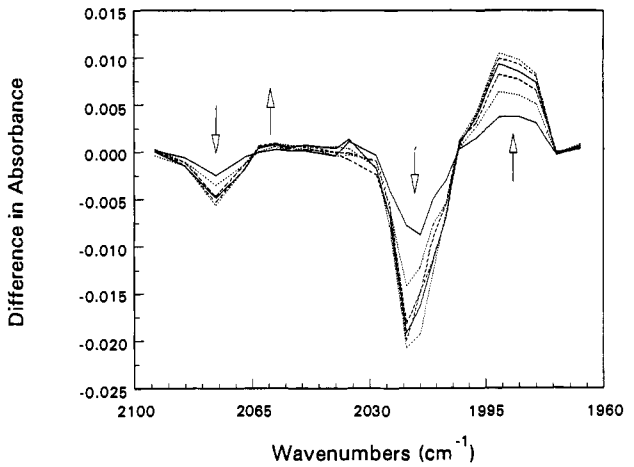

Figure 4. Time-resolved diode laser flow cell difference spectrum for ~40 mTorr of $Fe(CO)_5$ and 95 Torr of C_3H_6 photolyzed at 248 nm. The time-resolved spectrum is obtained by subtracting a spectrum acquired at 40 ms from spectra obtained over a collection time of 40–1840 ms in 300-ms increments. The solid trace marks the first time increment. Arrows indicate the direction of the evolution of absorptions.

As shown by the time-resolved difference spectrum (Figure 4), subsequent to 248-nm photolysis of $Fe(CO)_5$ in the presence of C_3H_6, species II decays to form species III with bands at 2060 and 1988 cm^{-1}. As seen in the figure for ~40 mTorr of $Fe(CO)_5$ and 95 Torr of C_3H_6 this takes place on a millisecond time scale. The absorption at 2060 cm^{-1} is more apparent in individual traces taken at this wavelength. Measurements of the rate of growth of species III as a function of C_3H_6 pressure, shown in Figure 5, leads to the determination of a rate constant of $(4.5 \pm 0.1) \times 10^{-16}$ cm^3 $molecules^{-1}$ s^{-1} for this process. The rate of decay of species II was the same as the rate of growth of species III.

Measurements of the rate of formation of species II with C_3D_6 yielded a bimolecular rate constant of $(2.6 \pm 0.2) \times 10^{-10}$ cm^3 $molecules^{-1}$ s^{-1} (Figure 3), virtually identical to that measured for C_3H_6. The propene-dependent decay of species II and formation of species III gave a rate constant of $(9.9 \pm 0.3) \times 10^{-16}$ cm^3 $molecules^{-1}$ s^{-1} for C_3D_6 (Figure 5). This rate constant is approximately twice as large as that for C_3H_6. The temperature dependence of the rate constants for the formation of species III is presented in Table 1.

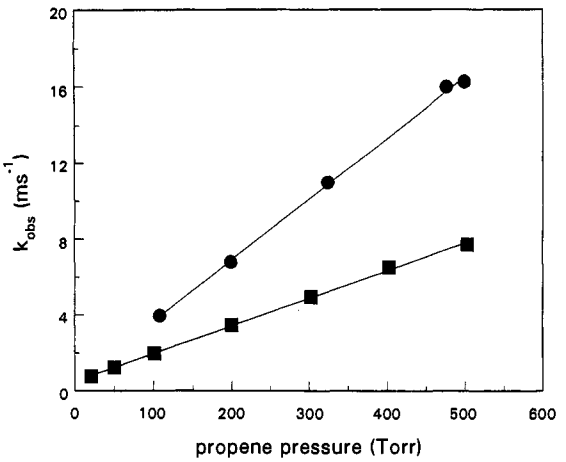

Figure 5. Plot of the pseudo-first-order rates at 296 K as a function of C_3H_6 (■) and C_3D_6 (●) pressure for the formation of species III monitored at 1985 cm^{-1}.

Table 1. Kinetic Parameters for the Decay of $HFe(CO)_3(\eta^3\text{-}C_3H_5)$ and the Formation of $Fe(CO)_3(C_3H_6)_2$

T (K)	k_{obs} (cm^3 $molecules^{-1}$ s^{-1}) × 10^{+16}	K_{eq} × 10^{+5}
	C_3H_6	
274	1.64 ± 0.06	0.9 ± 0.2
285	2.59 ± 0.09	1.4 ± 0.2
296	4.5 ± 0.3	2.5 ± 0.5
309	7.4 ± 0.1	4.1 ± 0.7
	C_3D_6	
273	3.6 ± 0.2	2.0 ± 0.4
285	6.76 ± 0.03	3.7 ± 0.6
296	9.9 ± 0.2	5.5 ± 0.9

The rate of formation of species III was also investigated in a high-pressure static cell. For pressures up to 11.4 atm, which is the vapor pressure of propene at 298 K, formation of species III is linear in C_3H_6 pressure and forms only as a result of the decay of species II. Additional data relevant to the mechanism proposed in the Discussion section are derived from measurements of the rate constants for the addition of C_3H_6 and C_2H_4 to $Fe(CO)_3(C_2H_4)$. Since mixtures of C_3H_6 and C_2H_4 were employed in these measurements, the rate constants were determined by fitting the appropriate decay rates to an equation of the form

$$\text{rate} = k_p[C_3H_6] + k_e[C_2H_4]$$

to obtain $(1.8 \pm 0.3) \times 10^{-11}$ and $(1.5 \pm 0.3) \times 10^{-11}$ cm^3 $molecules^{-1}$ s^{-1} for k_p and k_e, respectively.

IV. Discussion

A. Microsecond Time Scale: Formation of Species II. 1. Assignment. Photolysis of a mixture of $Fe(CO)_5$ and C_3H_6 at either 248 or 351 nm results in the C_3H_6-dependent decay of $Fe(CO)_3$ to generate species II with absorption bands at 2077 and 2011 cm^{-1}. To aid in identifying this and other species formed in these experiments, Figure 6 provides a collection of the known gas-phase and matrix absorption bands of compounds resulting from reactions of $Fe(CO)_3$ with C_3H_6. As will be discussed below, absorptions of the ethylene analogues of these compounds are also useful in making the assignments of the propene-containing compounds and are thus also included in Figure 6.

The positions and relative intensities of the bands of species II agree best with the matrix absorptions of $HFe(CO)_3(\eta^3\text{-}C_3H_5)$, taking into account the expected blue shift of absorption bands in the gas phase relative to the matrix, which are often in the

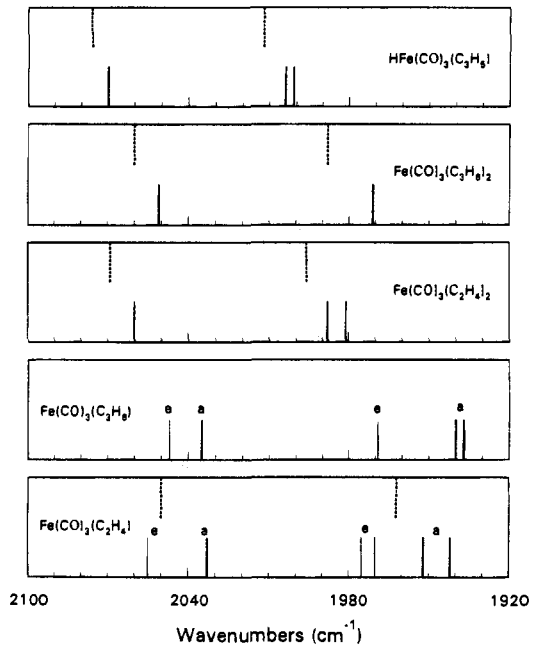

Figure 6. Comparison of gas phase (- - -) and matrix (—) assignments for $HFe(CO)_3(C_3H_5)$, $Fe(CO)_3(C_3H_6)_2$, $Fe(CO)_3(C_2H_4)_2$, $Fe(CO)_3(C_3H_6)$, and $Fe(CO)_3(C_2H_4)$. The letters "e" and "a" designate equatorial and apical isomers. Gas-phase assignments: $HFe(CO)_3(C_3H_5)$ and $Fe(CO)_3(C_3H_6)_2$, this study; $Fe(CO)_3(C_2H_4)_2$, ref 27; $Fe(CO)_3(C_2H_4)$, ref 31. Matrix assignments: $HFe(CO)_3(C_3H_5)$ and $Fe(CO)_3(C_3H_6)$ (Ar, 10 K), ref 15; $Fe(CO)_3(C_3H_6)_2$ and $Fe(CO)_3(C_2H_4)_2$ (MCH, 90 K), ref 28; $Fe(CO)_3(C_2H_4)$ (Ar, 10 K), ref 43. Ar = Argon, MCH = methylcyclohexane.

range of 10−20 cm^{-1}.[30] This species thus appears to result from the addition of propene to $Fe(CO)_3$ followed by the transfer of a β-hydrogen. Since C_2H_4 does not have β-hydrogens it was anticipated that spectra obtained under similar conditions, employing C_2H_4 as a ligand, would differ significantly from spectra obtained with C_3H_6. In the presence of C_2H_4, the decay of $Fe(CO)_3$ occurs at the same rate as the formation of two bands at 2045 and 1963 cm^{-1} which have previously been assigned to $Fe(CO)_3(\eta^2\text{-}C_2H_4)$. $Fe(CO)_3(\eta^2\text{-}C_2H_4)$ then rapidly decays at the same rate as a band at 1996 cm^{-1} grows in. This band has been previously assigned to $Fe(CO)_3(\eta^2\text{-}C_2H_4)_2$.[27] The differences in the reactive behaviors of C_3H_6 relative to C_2H_4 with $Fe(CO)_3$ are consistent with the work of Mitchner and Wrighton[14] involving the reaction of olefins with and without β-hydrogens with $Fe(CO)_3$, and further support the assignment of species II as $HFe(CO)_3(\eta^3\text{-}C_3H_5)$.

2. Mechanism. In the presence of C_3H_6, $Fe(CO)_3$ decays at the same rate as $HFe(CO)_3(\eta^3\text{-}C_3H_5)$ forms. The same rate of reaction was observed when He was added to the reaction mixture to achieve a total pressure of either ~25 or 50 Torr. Thus the reaction of $Fe(CO)_3 + C_3H_6$ is in the high-pressure limit with a rate constant for the overall reaction, $Fe(CO)_3 + C_3H_6 \rightarrow HFe(CO)_3(\eta^3\text{-}C_3H_5)$, of $(2.6 \pm 0.3) \times 10^{-10}$ cm^3 $molecules^{-1}$ s^{-1}. Reactions of $Fe(CO)_3$ with perdeuterated propene (C_3D_6) yielded a rate constant of $(2.6 \pm 0.2) \times 10^{-10}$ cm^3 $molecules^{-1}$ s^{-1}, virtually identical to that for C_3H_6.

The reaction mechanism in Scheme 1 involving the formation of $HFe(CO)_3(C_3H_5)$ by a β-hydrogen transfer process is consistent with all experimental observations. In this mechanism, $Fe(CO)_3(\eta^2\text{-}C_3H_6)$ is an intermediate between the separated reactants and the η^3-allyl species. Consistent with this picture, $Fe(CO)_3(\eta^2\text{-}C_3H_6)$ undergoes unimolecular rearrangement to form $HFe(CO)_3(\eta^3\text{-}C_3H_5)$ in a low-temperature matrix.[15]

(30) Poliakoff, M.; Weitz, E. *Acc. Chem. Res.* **1987**, *20*, 408.

Scheme 1

$$Fe(CO)_3 + C_3H_6 \xrightarrow{k_a} [Fe(CO)_3(\eta^2\text{-}C_3H_6)] \rightarrow HFe(CO)_3(\eta^3\text{-}C_3H_5)$$

As will be discussed in more detail in Section IV.B, this implies that $Fe(CO)_3(\eta^2\text{-}C_3H_6)$ is a local minimum in the potential energy surface for the $Fe(CO)_3 + C_3H_6$ system. Though $HFe(CO)_3(\eta^3\text{-}C_3H_5)$ is the first species that is *observed* subsequent to addition of C_3H_6 to $Fe(CO)_3$ in the present experiments, Scheme 1 indicates it is not the first species formed. $Fe(CO)_3(\eta^2\text{-}C_2H_4)$ is the initial product in the reaction of $Fe(CO)_3$ with C_2H_4, which does not have β-hydrogens.[31] This is consistent with $Fe(CO)_3(\eta^2\text{-}C_3H_6)$ as the initial product of the reaction of $Fe(CO)_3 + C_3H_6$ which is followed by rapid subsequent rearrangement of this species to form $HFe(CO)_3(\eta^3\text{-}C_3H_5)$. This mechanism is consistent with the generally accepted picture of C−H activation of olefins by transition metals involving initial formation of an η^2-alkene complex.[32]

Formation of a metal ligand complex by a simple associative pathway results in retention of the bond energy of the newly formed metal−ligand bond as internal excitation of the complex.[33] This internal energy must be relaxed to stabilize the complex. As indicated above, measurements of the rate of the reaction of $Fe(CO)_3 + C_3H_6$ were made at rare gas (He) pressures between 25 and 50 Torr where the rate constant for reaction of $Fe(CO)_3 + C_3H_6$ is in the high-pressure limit. However, even though 25 Torr is sufficient to suppress the dissociation of $Fe(CO)_3(\eta^2\text{-}C_3H_6)$ to $Fe(CO)_3$ and propene, it is likely that there remains significant internal excitation of the $Fe(CO)_3$−propene complex for a considerable period of time. Collisional vibrational relaxation of metal carbonyls and molecules of similar complexity typically occur with rate constants in the range of 10^{-12}−10^{-11} cm^3 $molecules^{-1}$ s^{-1}.[34] Even though vibrational deactivation is fast enough to stabilize the η^2-complex relative to dissociation, the stabilized η^2-complex may still have enough energy to very rapidly cross the barrier to form the η^3-species. As discussed below, it is likely that the rate constant for unimolecular rearrangement of even the *internally relaxed* complex exceeds 10^{10} s^{-1} at room temperature. Therefore, due to this extremely fast unimolecular rearrangement, the overall reaction to form the η^3-allylic species is rate-limited by the formation of the η^2-complex. This process has essentially the same rate for a perdeuterated propene as for propene. This would be expected for a rate-limited step involving formation of an η^2-adduct but would be surprising if the rate-limiting step were β-hydrogen transfer.

B. Millisecond Time Scale: Formation of Species III. 1. Assignment. Species II, $HFe(CO)_3(\eta^3\text{-}C_3H_5)$, reacts on a millisecond time scale, in the presence of a few hundred Torr of C_3H_6. The reaction product, designated as species III, has bands at 2060 and 1988 cm^{-1} (Figure 4). The propene dependence of the rate of formation of species III suggests that species III is a bis-propene adduct. Figure 6 shows that the bands for species III are in good agreement with the MCH matrix absorptions for $Fe(CO)_3(\eta^2\text{-}C_3H_6)_2$, taking into account typical matrix shifts. The absorption at 2060 cm^{-1} is expected to be much weaker than the absorption at 1988 cm^{-1}. In a MCH matrix the ratio of absorbances of these bands is reported as

(31) Hayes, D. M.; Weitz, E. *J. Phys. Chem.* **1991**, *95*, 2723.

(32) (a) Hill, C. L., Ed. *Activation and Functionalization of Alkanes*; Wiley: New York, 1989. (b) Parshall, G. W. *Homogeneous Catalysis*; Wiley: New York, 1980; Chapter 7.

(33) (a) Gravelle, S. J.; Weitz, E. *J. Am. Chem. Soc.* **1990**, *112*, 7839. (b) Gravelle, S. J.; Weitz, E. *J. Phys. Chem.* **1993**, *97*, 5272.

(34) (a) Bray, R. G.; Seidler, P. F.; Gethner, J. S.; Woodin, R. L. *J. Am. Chem. Soc.* **1986**, *108*, 1312. (b) Fletcher, T. R.; Rosenfeld, R. N. *J. Am. Chem. Soc.* **1985**, *107*, 2203.

Scheme 2

$$HFe(CO)_3(\eta^3\text{-}C_3H_5) \underset{k_1}{\overset{k_2}{\rightleftharpoons}} Fe(CO)_3(\eta^2\text{-}C_3H_6) \xrightarrow{k_+[C_3H_6]} Fe(CO)_3(\eta^2\text{-}C_3H_6)_2$$

11:1.[28] The absorptions of species III are also comparable with those of $Fe(CO)_3(\eta^2\text{-}C_2H_4)_2$. Based on these observations, species III is assigned as $Fe(CO)_3(\eta^2\text{-}C_3H_6)_2$.

2. Mechanism. A plausible mechanism for the formation of $Fe(CO)_3(\eta^2\text{-}C_3H_6)_2$ that is consistent with all available data is shown in Scheme 2.

Once formed, the η^3-allylic species is in equilibrium with the η^2-propene complex which can react with another propene to form the bis-propene species. The decay of $Fe(CO)_3(\eta^2\text{-}C_3H_6)_2$ is not included in Scheme 2 since it is stable on a much longer time scale than the other species in the scheme (*vide infra*). Reversible interconversion between η^2- and η^3-complexes is generally invoked as a key step in olefin isomerization catalyzed by many transition metal complexes,[11] including iron carbonyl.[13,14] Consistent with this picture, an equilibrium between η^2- and η^3-complexes has been observed in low-temperature solutions by ^1H NMR.[35] In further support of this mechanism, a recent study of $Cp^*Ir(\eta^3\text{-}C_3H_5)(H)$ shows that the reactions of this η^3-allylic hydride complex with arenes and alkanes proceed by the reversible formation of $Cp^*Ir(\eta^2\text{-}C_3H_6)$.[8]

A closed form solution for the kinetics of formation of $Fe(CO)_3(C_3H_6)_2$, in the context of Scheme 2, can be obtained by application of the steady state approximation to $[Fe(CO)_3(\eta^2\text{-}C_3H_6)]$. This leads to

$$k_{obs} = \frac{k_2 k_+ [C_3H_6]}{k_1 + k_+ [C_3H_6]} \quad (1)$$

where k_{obs} is the observed rate of formation of $Fe(CO)_3(\eta^2\text{-}C_3H_6)_2$, which is the same as the rate of decay of $HFe(CO)_3(\eta^3\text{-}C_3H_5)$. Under conditions where $k_1 \gg k_+[C_3H_6]$, *i.e.*, the reaction

$$Fe(CO)_3(C_3H_6) \xrightarrow{k_1} HFe(CO)_3(C_3H_5)$$

is much faster than addition of C_3H_6 to $Fe(CO)_3(\eta^2\text{-}C_3H_6)$, (1) becomes

$$k_{obs} = K_{eq} k_+ [C_3H_6] \quad (2)$$

where $K_{eq} = k_2/k_1$ is the equilibrium constant for the process

$$HFe(CO)_3(\eta^3\text{-}C_3H_5) \underset{k_1}{\overset{k_2}{\rightleftharpoons}} Fe(CO)_3(\eta^2\text{-}C_3H_6) \quad (3)$$

Thus, when $k_1 \gg k_+[C_3H_6]$, k_{obs} will depend linearly on $[C_3H_6]$, as observed, and a plot of k_{obs} as a function of $[C_3H_6]$ will yield a slope of $K_{eq}k_+$.

To obtain K_{eq} from the slope, k_+, the rate constant for addition of propene to $Fe(CO)_3(\eta^2\text{-propene})$ must be known. As discussed above, k_+ could not be measured directly in these experiments because the hydrogen transfer process in Scheme 2 that competes with this associative process is so rapid. However, k_+ can be estimated based on the rate constants for the addition of C_2H_4 and C_3H_6 to $Fe(CO)_3(\eta^2\text{-}C_2H_4)$. These rate constants were measured as (1.5 ± 0.3) and $(1.8 \pm 0.3) \times 10^{-11}$ cm^3 molecules^{-1} s^{-1} at room temperature, respectively.

(35) Barnhart, T. M.; De Fellippis, J.; McMahon, R. J. *Angew. Chem., Int. Ed. Engl.* **1993**, *32*, 1073.

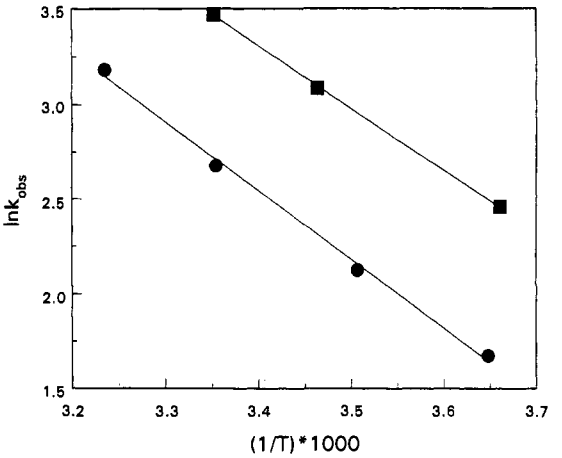

Figure 7. The Van't Hoff plots used to determine ΔH and ΔS for the process $HFe(CO)_3(C_3H_5) \rightarrow Fe(CO)_3(C_3H_6)$ for C_3H_6 (●) and C_3D_6 (■).

Since there is virtually no difference in the magnitude of these rate constants for ethylene versus propene, it is reasonable to assume that these rate constants will also not be significantly different if propene rather than ethylene is initially bound to $Fe(CO)_3$. Thus k_+ is estimated as 1.6×10^{-11} cm^3 molecules^{-1} s^{-1}. Within experimental error the rate constant for addition of C_2H_4 to $Fe(CO)_3(\eta^2\text{-}C_2H_4)$ is independent of temperature from 295 to 318 K. The temperature independence of the rate constant for addition of olefins to coordinatively unsaturated metal centers has, to date, been a general observation for the addition of small ligands to coordinatively unsaturated metal carbonyls in the gas phase.[36] Thus, k_+ is also very likely to be temperature independent. If the second propene adds to $Fe(CO)_3(C_3H_6)$ as an η^2-ligand then a minimal kinetic isotope would be expected for k_+, consistent with what is observed. The set of experimentally determined values for $K_{eq}k_+$ (k_{obs}) and calculated values for K_{eq} at different temperatures for C_3H_6 and C_3D_6 are shown in Table 1.

The enthalpy and entropy differences between $HFe(CO)_3(\eta^3\text{-}C_3H_5)$ and $Fe(CO)_3(\eta^2\text{-}C_3H_6)$ can be determined from the variation of K_{eq} with temperature. The van't Hoff plot shown in Figure 7 yields $\Delta H = 7.2 \pm 0.6$ kcal mol^{-1}, $\Delta S = 3 \pm 2$ cal K^{-1} mol^{-1} for C_3H_6 and $\Delta H = 6.5 \pm 0.4$ kcal mol^{-1}, $\Delta S = 2 \pm 1$ cal K^{-1} mol^{-1} for C_3D_6. Based on Table 1, at room temperature the equilibrium isotope effect, $K_{eq}(C_3D_6)/K_{eq}(C_3H_6)$, is 2.2 ± 0.1. This isotope effect is consistent with the change in nature of a normal mode in $HFe(CO)_3(\eta^3\text{-}C_3H_5)$, $(DFe(CO)_3(\eta^3\text{-}C_3D_5))$ associated with the metal hydride (deuteride) vibration, relative to a normal mode in $Fe(CO)_3(\eta^2\text{-}C_3H_6)$, $(Fe(CO)_3(\eta^2\text{-}C_3D_6))$ that is associated with the substantially higher-frequency C−H (C−D) vibration. McGhee and Bergman observed a similar isotope effect for the equilibrium between $Cp^*Ir(\eta^3\text{-}C_3H_5)(H)$ and $Cp^*Ir(\eta^2\text{-}C_3H_6)$ relative to their deuterated analogues,[8] providing further support of the mechanism in Scheme 2.

Equation 1 predicts that in the limit of very high propene pressure ($k_1 \ll k_+[C_3H_6]$), k_{obs} will no longer be linear in $[C_3H_6]$ and will approach k_2. However, over the experimental range of propene pressure, which was limited by the vapor pressure of propene, which is 11.4 atm at room temperature, k_{obs} remains linearly dependent on $[C_3H_6]$. This indicates that over this pressure range $k_1 > k_+[C_3H_6]$. Another indicator that the rate of addition of propene to $Fe(CO)_3(C_3H_6)$ does not successfully compete with the unimolecular rearrangement of $Fe(CO)_3(C_3H_6)$

(36) (a) Bogdan, P. C.; Wells, J. R.; Weitz, E. *J. Am. Chem. Soc.* **1991**, *113*, 1294. (b) Wells, J. R.; House, P. G.; Weitz, E. *J. Phys. Chem.* **1994**, *98*, 8343.

to $HFe(CO)_3(C_3H_5)$ is the absence of a response time limited rise of $Fe(CO)_3(\eta^2\text{-}C_3H_6)_2$ at high propene pressure. This initial rise would be present if propene could add to the *initially* generated $Fe(CO)_3(C_3H_6)$ before it *initially* converted to $HFe(CO)_3(C_3H_5)$. However, no fast initial component was observed for either propene or perdeuteropropene and under experimental conditions $Fe(CO)_3(\eta^2\text{-}C_3H_6)_2$ appears to only form from the addition of C_3H_6 to $Fe(CO)_3(\eta^2\text{-}C_3H_6)$ that is in equilibrium with $HFe(CO)_3(\eta^3\text{-}C_3H_5)$. These observations imply that even for 11.4 atm (~8700 Torr) of propene k_1 is still much larger than $k_+[C_3H_6]$, *i.e.*, the rate for the unimolecular rearrangement is much faster than the rate of addition of C_3H_6 to $Fe(CO)_3(\eta^2\text{-}C_3H_6)$. Since $k_+ \sim 1.6 \times 10^{-11}$ cm^3 molecules^{-1} s^{-1}, a lower limit of approximately 10^{10} s^{-1} can be determined for k_1 at room temperature. If a preexponential of 10^{13} s^{-1} is assumed, typical of thermal unimolecular rearrangements with constrained transition states,[37] an activation enthalpy ΔH_f for the unimolecular rearrangement can be estimated to be ≤ 3.5 kcal mol^{-1}. Similar statements apply to the deuterated analogues. It should be noted that k_1 is the rate constant for a reaction that is anticipated to involve a change in spin multiplicity.[23] Such reactions have typically exhibited preexponentials that are small compared to analogous spin conserving processes. However, a decrease in the preexponential, which is possible for a formally spin disallowed process, leads to a smaller activation energy, still consistent with the stated upper limit.

It is now worth commenting on why addition of C_3H_6 does not efficiently compete with the initial isomerization step for $Fe(CO)_3(C_3H_6)$ but does form by reaction with $Fe(CO)_3(C_3H_6)$ that is in equilibrium with $HFe(CO)_3(C_3H_5)$. In the initial reaction step, subsequent to formation of $Fe(CO)_3(C_3H_6)$, the data demonstrate that isomerization is much faster than the addition of a second propene. However, once an equilibrium is established, there remains a small but finite equilibrium concentration of $Fe(CO)_3(C_3H_6)$. The data in Table 1 indicate that this concentration is approximately 10^{-5} of the initially produced $Fe(CO)_3(C_3H_6)$. However, despite the smaller concentration there is a much longer time window over which reaction can occur than for the initial concentration of $Fe(CO)_3(C_3H_6)$. The measurement of a *phenomenological* rate constant for formation of $Fe(CO)_3(C_3H_6)_2$ of 4.5×10^{-16} cm^3 molecules^{-1} s^{-1} (k_+K_{eq}) represents the effect of the reduced equilibrium concentration of $Fe(CO)_3(C_3H_6)$ on the expected *microscopic* rate constant for addition of C_3H_6 to $Fe(CO)_3(C_3H_6)$ of $\sim 1.6 \times 10^{-11}$ cm^3 molecules^{-1} s^{-1}.

It is interesting to note that in rare gas matrices at 10 K both $Fe(CO)_3(\eta^2\text{-}C_3H_6)$ and $HFe(CO)_3(\eta^3\text{-}C_3H_5)$ are observed following UV photolysis (260 ± 10 nm) of $Fe(CO)_4(\eta^2\text{-}C_3H_6)$.[15] Since the photon energy is much higher than the CO binding energy in $Fe(CO)_4(\eta^2\text{-}C_3H_6)$, the nascent $Fe(CO)_3(\eta^2\text{-}C_3H_6)$ must have an internal energy that is well in excess of the activation barrier of $\Delta H_f^{\ddagger} \leq 3.5$ kcal mol^{-1}. If vibrational relaxation did not compete with rearrangement, essentially all of the nascent $Fe(CO)_3(\eta^2\text{-}C_3H_6)$ would rearrange to form $HFe(CO)_3(\eta^3\text{-}C_3H_5)$. The fact that $Fe(CO)_3(\eta^2\text{-}C_3H_6)$ appears as a primary photoproduct implies that the rate of vibrational relaxation in matrices is comparable to that for unimolecular rearrangement. Since vibrational relaxation in condensed phases is typically on the order of picoseconds,[38] a plausible upper bound for the rate (which is equivalent to the rate constant for a unimolecular process) of β-hydrogen transfer is approximately 10^{12} s^{-1}. This appears to be qualitatively consistent with the present gas-phase results, despite the potentially over-simplified picture of the dynamics in a matrix environment.

(37) Robinson, P. J.; Holbrook, K. A. *Unimolecular Reactions*; Wiley-Interscience: London, 1972.

(38) Yardley, J. T. *Introduction to Molecular Energy Transfer*; Academic: New York, 1980.

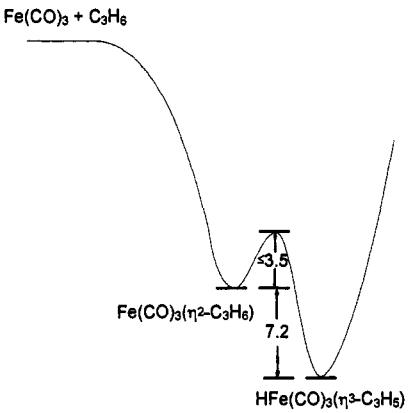

Figure 8. A diagram of the change in enthalpy along the reaction coordinate for β-hydrogen transfer in the $Fe(CO)_3$–propene system.

Both the lower limit for the rate constant, $k_1 \geq 10^{10}$ s^{-1}, and upper limit for the activation enthalpy, $\Delta H_f^{\ddagger} \leq 3.5$ kcal mol^{-1}, indicate that the β-hydrogen transfer process is extremely facile. This conclusion is consistent with a number of observations reported in the literature. Barnhart *et al.* observed that the hydrogen transfer occurs thermally at 5 K in matrices.[15] In fact, if this reaction proceeds by surmounting a barrier, this result implies a much smaller barrier than 3.5 kcal mol^{-1}. An activation energy significantly in excess of 100 cal mol^{-1} would preclude the observation of significant isomerization on the operable time scale. However, tunneling could also significantly contribute to the observed rate of reaction. In related studies of C–H activation of alkanes by photolysis of $Cp^*Rh(CO)_2$ in liquid rare gases, Moore and co-workers reported activation enthalpies of $\Delta H^{\ddagger} = 4\text{–}5$ kcal mol^{-1} for the reaction,[20]

$$Cp^*Rh(CO)(R\text{–}H) \rightarrow Cp^*Rh(CO)(R)(H)$$

In a study of the photochemistry of $CpM(CO)_3Et$ (M = Mo and W), it was also concluded that the β-hydrogen transfer process,

$$CpM(CO)_2Et \rightarrow CpM(CO)_2(C_2H_4)(H)$$

does not involve significant activation barriers.[18]

From ΔH, the enthalpy difference between $HFe(CO)_3(\eta^3\text{-}C_3H_5)$ and $Fe(CO)_3(\eta^2\text{-}C_3H_6)$, and $\Delta H_f^{\ddagger}$, the activation enthalpy for hydrogen transfer, an activation enthalpy $\Delta H_b^{\ddagger} = \Delta H + \Delta H_f^{\ddagger}$ that is between 8.5 and 12 kcal mol^{-1} can be derived for the back reaction, $HFe(CO)_3(\eta^3\text{-}C_3H_5) \rightarrow Fe(CO)_3(\eta^2\text{-}C_3H_6)$. On the basis of the lifetime of $HFe(CO)_3(\eta^3\text{-}C_3H_5)$ in low-temperature solutions, Barnhart *et al.* estimated the activation free energy for the same process to be 9–12 kcal mol^{-1},[35] consistent with the activation free energy calculated from our results.

As previously pointed out, the reactions in Scheme 1 are anticipated to involve changes in spin multiplicity and therefore involve multiple potential energy surfaces.[17] Figure 8 is a schematic diagram of the enthalpy along the reaction coordinate which does not explicitly depict the presence of multiple potential energy surfaces.

Alternative Mechanism. An alternative mechanism for the formation of $Fe(CO)_3(\eta^2\text{-}C_3H_6)_2$, which is also consistent with the observed kinetics, involves the "associative" addition of propene to the η^3-allylic species.

$$HFe(CO)_3(\eta^3\text{-}C_3H_5) + C_3H_6 \rightarrow [\text{transition state}]^{\ddagger} \rightarrow Fe(CO)_3(\eta^2\text{-}C_3H_6)_2 \quad \text{(a)}$$

Reaction a predicts that the rate of formation of $Fe(CO)_3(\eta^2\text{-}C_3H_6)_2$, or decay of $HFe(CO)_3(\eta^3\text{-}C_3H_5)$, will depend linearly on $[C_3H_6]$, in agreement with the experimental observations. In the context of reaction a, the slope in Figure 5 gives the bimolecular rate constant for this reaction and the change in the rate constant for the perdeuterated relative to protonated species relates directly to the *kinetic* isotope effect. In this case that would be $k^D/k^H = 2.2 \pm 0.1$ ($k^H/k^D = 0.45$). With this interpretation, the kinetic isotope effect for this mechanism would be similar to the equilibrium isotope effect for the equilibrium between $Cp^*Ir(\eta^3\text{-}C_3H_5)(H)$ and $Cp^*Ir(\eta^2\text{-}C_3H_6)$.[8] This suggests that in the transition state for reaction a, the $HFe(CO)_3(\eta^3\text{-}C_3H_5)$ fragment has rearranged to a structure very close to $Fe(CO)_3(\eta^2\text{-}C_3H_6)$. Thus, the transition state for reaction a could be formulated as $[Fe(CO)_3(\eta^2\text{-}C_3H_6)\cdots C_3H_6]^{\ddagger}$ where the dots refer to an interaction between $Fe(CO)_3(\eta^2\text{-}C_3H_6)$ and the entering C_3H_6 prior to formation of the second $Fe\text{-}(\eta^2\text{-}C_3H_6)$ bond. By microscopic reversibility, the back reaction proceeds by the same transition state,

$$Fe(CO)_3(\eta^2\text{-}C_3H_6)_2 \rightarrow [Fe(CO)_3(\eta^2\text{-}C_3H_6)\cdots C_3H_6]^{\ddagger} \rightarrow HFe(CO)_3(\eta^3\text{-}C_3H_5) + C_3H_6 \quad \text{(b)}$$

Before the substantial extension of one of the $Fe\text{-}(\eta^2\text{-}C_3H_6)$ bonds, the bonding of the other propene ligand will not change significantly. Thus, in the transition state the interaction between the metal center and the leaving C_3H_6 is weak. As will be discussed in section IV.C, the activation enthalpy for reaction b is the same within experimental error as that of the dissociative loss of C_2H_4 from $Fe(CO)_3(\eta^2\text{-}C_2H_4)_2$. This further suggests that in the transition state for reactions a and b the interaction between the metal center and the entering or the leaving C_3H_6 is negligible. That is, the transition state is virtually two separated species, $Fe(CO)_3(\eta^2\text{-}C_3H_6) + C_3H_6$. This argument leads to a situation where even if an "associative" addition mechanism to $HFe(CO)_3(C_3H_5)$ were operative, it would occur by a microscopic mechanism that is effectively the same as that proposed in Scheme 1. However in Scheme 1, $Fe(CO)_3(\eta^2\text{-}C_3H_6)$ is present in equilibrium with $HFe(CO)_3(C_3H_5)$ while in the "associative" addition mechanism $HFe(CO)_3(C_3H_5)$ only converts to a transition state that looks like $Fe(CO)_3(\eta^2\text{-}C_3H_6)$ in the presence of C_3H_6. While we cannot rule out this "associative mechanism" based on the data, we favor the mechanism in Scheme 1 based on the mechanism reported in the literature for olefin isomerization[13,14] and β-hydride transfer processes in analogous compounds.[8,35]

Another mechanism that is "associative," involving formation of a formally $20e^-$ intermediate, is also consistent with the observed kinetics. However, there is no precedent for such an associative $20e^-$ mechanism in the literature. Additionally, if the observed kinetics were ascribed to such a mechanism it would lead to the prediction of an activation energy for the addition of a second propene to the η^3 complex of ~8 kcal mol^{-1}, seemingly far too small for a process that would involve significant steric crowding around the metal center and thus significant interligand repulsion. Thus, we feel this mechanism can be excluded from consideration.

C. Long Time Scale Decay of $Fe(CO)_3(\eta^2\text{-}C_3H_6)_2$. $Fe(CO)_3(\eta^2\text{-}C_3H_6)_2$ decays on a time scale that is longer than can be conveniently followed by either the CO or diode laser probes. However, its decay, which occurs on a time scale of a few tenths of a second to a few minutes depending on the C_3H_6 and CO pressures, can be conveniently followed by FTIR. In the presence of added CO, the decay rate of $Fe(CO)_3(\eta^2\text{-}C_3H_6)_2$ is the same as the rate of growth of $Fe(CO)_4(\eta^2\text{-}C_3H_6)$ which in turn decays with the concurrent formation of $Fe(CO)_5$. Scheme 3 presents a plausible mechanism for this process.

Scheme 3

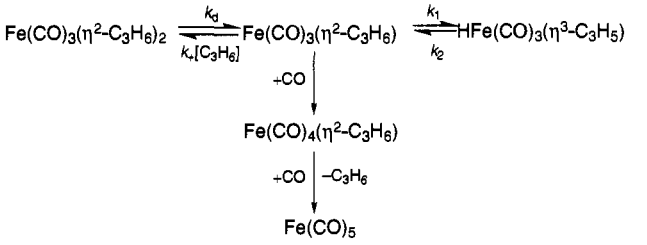

Scheme 4

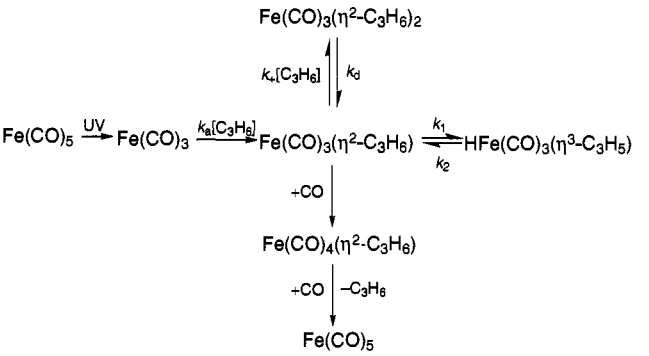

The rate constant for dissociative loss of C_3H_6 from $Fe(CO)_3(\eta^2\text{-}C_3H_6)_2$, k_d, can be evaluated from the decay rate of $Fe(CO)_3(\eta^2\text{-}C_3H_6)_2$ using a now well documented procedure,[17] given that all other relevant rate constants are known or can be estimated from data on the analogous C_2H_4 system. Using this procedure, k_d is estimated to be ~10 s^{-1} at room temperature. The preexponential for dissociation of C_2H_4 from $Fe(CO)_3(\eta^2\text{-}C_2H_4)_2$ is 2.6×10^{14} s^{-1}.[39] Assuming the same preexponential for C_3H_6 leads to a C_3H_6 bond enthalpy of ~19 kcal mol^{-1} in $Fe(CO)_3(\eta^2\text{-}C_3H_6)_2$, similar to 21 ± 2 kcal mol^{-1} for the loss of C_2H_4 from $Fe(CO)_3(\eta^2\text{-}C_2H_4)_2$ which occurs by a dissociative mechanism. As discussed in Section IV.B, this agreement between these two bond energies is consistent with a dissociative loss mechanism for C_3H_6 from $Fe(CO)_3(\eta^2\text{-}C_3H_6)_2$.

D. Overall Mechanism. The mechanism in Scheme 4 is a composite of the mechanisms considered in the prior sections. UV photolysis of $Fe(CO)_5$ produces $Fe(CO)_3$ which reacts with C_3H_6 at a near gas kinetic rate to form $Fe(CO)_3(\eta^2\text{-}C_3H_6)$. $Fe(CO)_3(\eta^2\text{-}C_3H_6)$ undergoes unimolecular hydrogen transfer to form the η^3-allyl species, $HFe(CO)_3(\eta^3\text{-}C_3H_5)$, at a rate $\geq 10^{10}$ s^{-1}. As a result of the extremely fast unimolecular rearrangement of $Fe(CO)_3(\eta^2\text{-}C_3H_6)$, addition of the second C_3H_6 to $Fe(CO)_3(\eta^2\text{-}C_3H_6)$, formed initially by reaction of $Fe(CO)_3$ with C_3H_6, cannot compete effectively with the initial β-hydrogen transfer process to form $HFe(CO)_3(C_3H_5)$. However, $HFe(CO)_3(\eta^3\text{-}C_3H_5)$ is in equilibrium with $Fe(CO)_3(\eta^2\text{-}C_3H_6)$ and rearranges to form this species with a rate constant that is five orders of magnitude smaller than that for the forward reaction. In the presence of C_3H_6, $Fe(CO)_3(\eta^2\text{-}C_3H_6)$ in equilibrium with $HFe(CO)_3(\eta^3\text{-}C_3H_5)$ can be trapped to form $Fe(CO)_3(\eta^2\text{-}C_3H_6)_2$. The

(39) House, P. G.; Weitz, E. Manuscript in preparation.
(40) Whetten, R. L.; Fu, K.-J.; Grant, E. R. *J. Am. Chem. Soc.* **1982**, *104*, 4270.
(41) Whetten, R. L.; Fu, K.-J.; Grant, E. R. *J. Chem. Phys.* **1982**, *77*, 3769.

rate constant for decay of $Fe(CO)_3(\eta^2\text{-}C_3H_6)_2$, by the dissociative loss of C_3H_6, leads to an estimate for the bond enthalpy for $Fe(CO)_3(\eta^2\text{-}C_3H_6)-(\eta^2\text{-}C_3H_6)$ of ~19 kcal mol^{-1}. In the absence of excess ligand, any of the coordinatively unsaturated species can, in principle, react with parent to form polynuclear iron-contained species which are likely to be involatile.[42] This pathway is not explicitly included in Scheme 4.

From Scheme 5 and Figure 8 the energy of the $Fe(CO)_3\text{-}(\eta^3\text{-}C_3H_5)$ bond can, in principle, be calculated using the following equation with the energy of the separated $Fe(CO)_3$ and C_3H_6 molecules as the reference level,:

$$H(CO)_3Fe-(\eta^3\text{-}C_3H_5) = (H-C_3H_5) - (H-Fe) + ((\eta^2\text{-}C_3H_6)-Fe(CO)_3) + (Fe(CO)_3(C_3H_6)-HFe(CO)_3(\eta^3\text{-}C_3H_5)) \quad (4)$$

The dissociation energy for a propene β-hydrogen is approximately 88 kcal/mol.[44] The energy difference between $Fe(CO)_3(C_3H_6)$ and $HFe(CO)_3(\eta^3\text{-}C_3H_5)$ has been measured in this study to be ~7 kcal/mol. The other energies can only be estimated. The bond energy for the loss of C_3H_6 from $Fe(CO)_3\text{-}(C_3H_6)_2$ has been estimated in this study to be 19 kcal/mol. Though the bond energy for C_3H_6 in $Fe(CO)_3(C_3H_6)$ is not necessarily the same as in the bis-olefin complex, we take 19 kcal/mol as a reasonable value for the bond energy of propene in the mono-olefin complex. The final bond energy is that for H−Fe. This number has been measured for FeH as 37.5 kcal/mol.[45] However, this is for the Fe−H bond in diatomic FeH not the H−Fe bond in $HFe(CO)_3(C_3H_5)$. Nevertheless, this number provides the best currently available estimate for the desired bond energy. However, it should be noted that the H−Fe bond energy is relatively low compared to a typical metal hydride bond energy which is often quoted as being in the range of 60 kcal/mol.[46] Using these values as inputs leads to a bond energy of ~76 kcal/mol for the $(\eta^3\text{-}C_3H_5)$−Fe bond. This value is comparable to the bond energy of 79 kcal/mol for Fe bound to the Cp ligand $(\eta^5\text{-}C_5H_5)$ in ferrocene.[47]. Though this estimate makes it clear that $\eta^3\text{-}C_3H_5$ binds strongly to Fe, there is room for considerable error in this estimate with the largest source of error being the values used for the H−Fe and (C_3H_6)−Fe-$(CO)_3$ bonds. If the bond energy for the $\eta^3\text{-}C_3H_5$ ligand is comparable to that for $(\eta^5\text{-}C_5H_5)$ in ferrocene, this would seem to imply that the smaller C_3H_5 ligand can bind in a more energetically favorable geometry.

E. Mechanism for Iron Carbonyl-Catalyzed Isomerization of Olefins. Iron carbonyl-photocatalyzed isomerization of olefins has been extensively studied in both the condensed[13,14,28,40] and gas[41] phases. Photolysis generates a catalyst that is active at ambient temperatures. A mononuclear tricarbonyl iron unit, although not observed under catalytic conditions, has been proposed as a reservoir for the catalytic cycle shown in Scheme 5.[40] In the iron carbonyl-photocatalyzed isomerization of pentene, at a pressure of a few hundred Torr, the lifetime of the catalyst is ~0.2 s.[41] Under similar conditions with propene, the only species that are stable on this time scale are $Fe(CO)_3\text{-}(\eta^2\text{-}C_3H_6)_2$ and $Fe(CO)_4(\eta^2\text{-}C_3H_6)$. The mono-olefin species is an unlikely active catalytic species since it loses propene very slowly and virtually all proposed catalytic intermediates require two coordination sites that can participate in the catalytic cycle. Thus, our findings provide direct support for the tricarbonyl iron unit as an active catalytic species with $Fe(CO)_3(\eta^2\text{-olefin})_2$ as the "reservoir" species. This species has also been implicated in the catalytic hydrogenation of olefins.[31,42]

Scheme 5

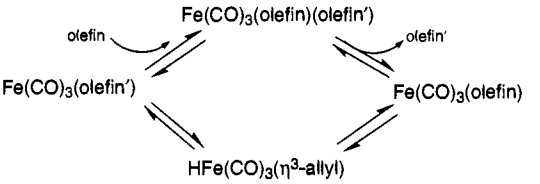

V. Conclusion

The overall observations of this study are summarized in Scheme 4. UV photolysis of $Fe(CO)_5$ produces $Fe(CO)_3$, a coordinatively unsaturated fragment with two vacant coordination sites. $Fe(CO)_3$ reacts with C_3H_6 at a near gas kinetic rate to form $Fe(CO)_3(\eta^2\text{-}C_3H_6)$. $Fe(CO)_3(\eta^2\text{-}C_3H_6)$ undergoes unimolecular β-hydrogen transfer to form the η^3-allyl species, $HFe(CO)_3(\eta^3\text{-}C_3H_5)$. The lower limit for the rate constant for β-hydrogen transfer in the internally relaxed system is 10^{10} s^{-1} at room temperature. Initially formed $Fe(CO)_3(\eta^2\text{-}C_3H_6)$ is expected to be internally excited, which could further enhance the rate of unimolecular isomerization to $HFe(CO)_3(\eta^3\text{-}C_3H_5)$, which is the thermodynamically more stable isomer. Due to this very facile unimolecular rearrangement of $Fe(CO)_3(\eta^2\text{-}C_3H_6)$, addition of the second C_3H_6 to the initially formed $Fe(CO)_3(\eta^2\text{-}C_3H_6)$ cannot compete effectively with the β-hydrogen transfer process. The data are consistent with $HFe(CO)_3(\eta^3\text{-}C_3H_5)$ being in equilibrium with $Fe(CO)_3(\eta^2\text{-}C_3H_6)$ with an equilibrium constant $K_{eq} = k_2/k_1 = 2.4 \times 10^{-5}$ at room temperature. The $Fe(CO)_3(\eta^2\text{-}C_3H_6)$ that is in equilibrium with $HFe(CO)_3(\eta^3\text{-}C_3H_5)$ can then be trapped by C_3H_6 to form $Fe(CO)_3(\eta^2\text{-}C_3H_6)_2$. The phenomenological rate constant for this process is given by $K_{eq}k_+$ where k_+ is the rate constant for addition of C_3H_6 to $Fe(CO)_3(C_3H_6)$. $Fe(CO)_3(\eta^2\text{-}C_3H_6)_2$ has a bond enthalpy for loss of a propene ligand of ~19 kcal mol^{-1}. Its decay in the presence of CO leads to the production of $Fe(CO)_4(C_3H_6)$ which is even more stable and effectively removes iron photofragments from further participation in the reaction scheme under study.

The present study has significant implications for the generally accepted mechanism for transition metal catalyzed olefin isomerization which is shown in Scheme 5. For propene and iron carbonyl, the rate constants for the major steps in the proposed mechanism have been obtained or estimated. The results provide evidence that $Fe(CO)_3(C_3H_6)_2$ is the "reservoir" species for the catalytically active iron carbonyl species and show that the major steps in the cycle are kinetically and thermodynamically plausible, thus providing firm support for this mechanism of olefin isomerization involving an η^3-allyl hydride intermediate.

Acknowledgment. We acknowledge support of this work by the National Science Foundation under Grant No. CHE-9024509. One of us (G.T.L.) acknowledges a Dow, Department of Education (GANN) Fellowship.

JA951545+

(42) Wells, J. R.; Weitz, E. *J. Phys. Chem.* **1993**, *97*, 3084.
(43) Barnhart, T. M.; Fenske, R. F.; McMahon, R. J. *Inorg. Chem.* **1992**, *31*, 2679.
(44) Morrison, R. T.; Boyd, R. N. *Organic Chemistry*, 3rd ed.; Allyn and Bacon: Boston, 1973.
(45) Schultz, R. H.; Armentrout, P. B. *J. Chem. Phys.* **1991**, *94*, 2262.
(46) Halpern, J. *Inorg. Chim. Acta* **1985**, *100*, 41.
(47) Richardson, D. E.; Christ, C. S., Jr.; Sharpe, P.; Ryan, M. F.; Eyler, J. R. *Bonding and Energetics in Organometallic Chemistry*; Marks, T. J., Ed.; ACS Symposium Series 428; American Chemical Society: Washington, DC, 1990.